Proceedings of the XVII ECSMGE-2019
Geotechnical Engineering foundation of the future
ISBN 978-9935-9436-1-3

doi: 10.32075/17ECSMGE-2019-0673

XVII European Conference
ECSMGE 2019
Reykjavik
on Soil Mechanics
and Geotechnical Engineering

A novel technique for simulating submarine landslides in geo-centrifuge

Une nouvelle technique de simulation de glissements de terrain sous-marins en géo-centrifugeuse

W. Zhang
Department of Geo-Sciences and Engineering, TU Delft, Delft, The Netherlands

A. Askarinejad
Department of Geo-Sciences and Engineering, TU Delft, Delft, The Netherlands

ABSTRACT: Souring erosion around structural elements on the seabed, sediment transport, dredging and other similar anthropogenic offshore activities can cause an increase of seabed angle, hence, sudden instabilities can be triggered. The details of a novel actuator designed with a tilting mechanism for simulating the process of seabed angle rise in centrifuge are presented. A strongbox equipped with a fluidization system was used to prepare a very loose saturated sand sample which is similar to the naturally deposited sands and has a high potential to liquefy. The measured excess pore pressures of a 10g test are discussed. Results show that sand liquefaction could be triggered statically as a result of gradually increasing of slope angle.

RÉSUMÉ: L'érosion généralisée autour des éléments structurels du fond marin, le transport de sédiments, le dragage et d'autres activités anthropiques en mer similaires peuvent entraîner une augmentation de l'angle du fond marin, ce qui peut entraîner une instabilité soudaine. Les détails d'un nouvel actionneur conçu avec un mécanisme de basculement pour simuler le processus d'élévation de l'angle du fond marin dans une centrifugeuse sont présentés. Un coffre-fort équipé d'un système de fluidisation a été utilisé pour préparer un échantillon de sable saturé très lâche, similaire aux sables déposés naturellement et qui a un fort potentiel de liquéfaction. Les pressions interstitielles mesurées lors d'un test de 10g sont discutées. Les résultats montrent que la liquéfaction du sable pourrait être déclenchée de manière statique du fait de l'augmentation progressive de l'angle de la pente.

Keywords: Static Liquefaction; Submarine landslides; Centrifuge Modelling

1 INTRODUCTION

Seabed instabilities can damage or influence the stability of assets such as offshore platforms and pipelines. Submerged slope inclination can gradually rise as a result of toe erosion or top deposition (Kvalstad et al. 2001). The seabed erosion near the end of seabed protection layers of the Easter Scheldt Storm Surge barrier in the South Western part of the Netherlands is taking place due to strong currents (De Jager 2018). Static liquefaction can be triggered during this process and is reported as one of the main triggers for loosely packed granular materials under temporary undrained condition (Lade 1992; Silvis & Groot 1995; Jefferies & Been 2006; Masson et al. 2006). Sudden accumulation of excess pore pressure can reduce the effective stresses, hence, cause catastrophic failure.

Static liquefaction of saturated loose sands has been well studied by conducting undrained triaxial compression tests (e.g, Chu et al. 2003). However, a soil element test could only represent the soil behaviour of a "point" of soil mass in the field. The stress state and pore pressure change of a slope due to the elevation of slope angle is complex and difficult to be measured (De Groot et al. 2012). This calls for the application of physical modelling technique which could represent prototype soil mass properties.

Both small-/large-scale tests (1*g* tests) and centrifuge tests (N*g* tests) have been conducted in order to study the landslides behaviour and their influence on offshore structures; however, the triggering mechanism has not been taken into account in most of these studies (De Groot et al. 2012; Askarinejad et al. 2018). A Liquefaction Tank at TU Delft was developed for studying marine landslides induced by slope over-steepening (De Jager et al. 2017). While, the application of 1g tests' results is limited by the sample height, for instance, the highest sand layer could be made in the Liquefaction Tank is 1.5 m. The centrifuge technique can overcome this limitation. However, only limited tests have been done to study this problem using geotechnical centrifuges (e.g. Sassa & Sekiguchi 1999; Byrne et al. 2000; Maghsoudloo et al. 2017; Askarinejad et al. 2018). Hence, a novel tilting device has been designed to simulate the process of slope over-steepening and the potential subsequent flow slide in the centrifuge.

This paper presents the test setup made for simulating static liquefaction of submerged slopes triggered by slope over-steepening. A new method of preparing saturated loose sand for the purpose of centrifuge modelling of static liquefaction is introduced. Moreover, the evolution of pore water pressure inside a model soil layer subjected to steepening is discussed.

2 SAMPLE PREPARATION TECHNIQUE

Sample preparation techniques are of crucial importance for studying soil properties. In current practice, moist tamping, air pluviation and wet pluviation are commonly adopted for element tests in laboratory. The aim of these specimen reconstitution techniques is to simulate the sand mass in the field, for example to replicate the relative density or fabric of the soil. The sand resistance to liquefaction is sensitive to the initial soil properties which depend on the specimen reconstitution techniques. The moist tamping technique has the advantage of making loose samples, however, the samples' uniformity cannot be promised (Vaid et al. 1999). Della et al. (2009) found that samples made by the wet deposition method was more vulnerable to the liquefaction than those made the dry pluviation method.

For centrifuge modelling on static liquefaction, saturated samples are larger than that of element tests; besides, they are in a very loose state. Therefore, a sample preparation technique should take into account not only the sample properties but also any possible disturbance may be caused by placing the sample into the centrifuge carrier. The drizzle method could make saturated samples with relative densities smaller than 5% (Rietdijk et al. 2010). However, such a loose sample tends to be densified during the sample transportation. Askarinejad et al. (2018) prepared loose samples using the wet pluviation method. While it took 8 hours for making a sample with a volume of about 5500 cm^3.

As a more efficient alternative, the fluidization technique was applied in 1g tests by previous researchers (e.g. Spence & Guymer 1997; De Jager et al. 2017). Therefore, a strongbox was assembled in this study with a fluidization system aiming at preparing saturated loose sand samples. Furthermore, samples could be made after fixing the strongbox into the centrifuge carrier, hence no artificial disturbance

will be applied onto the samples before starting the centrifuge.

The design of the strongbox is illustrated in Figure 1**Error! Reference source not found.**, which was assembled with three aluminium plates at two short sides and bottom, and with two transparent Plexiglas sheets. The width and length of a sample are 134 mm and 355 mm, respectively; the sample height is adjustable up to a value of 110 mm, in model scale. The aluminium extension box on the top was used for preventing fluid over flow (further explained in the following section). Three pore pressure transducers (PPTs, MPXH6400A) were fixed on the fluidization filter, i.e. they are located at the base of the sample.

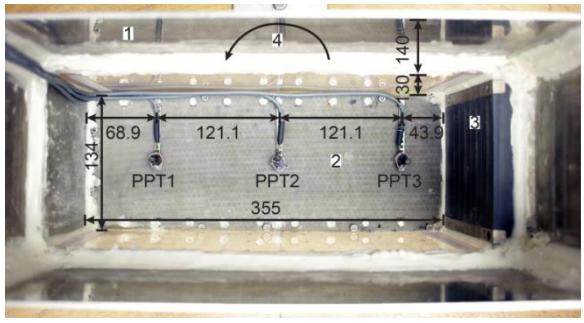

Figure 1. Top view of the newly developed strongbox with an integrated fluidization system at the base: 1) extension box; 2) fluidization filter; 3) PVC block; 4) tilting direction. (unit: mm, model scale)

The fluidization system was integrated into the base plate of the strong box. It is composed of a fluidization filter (Figure 1) and a pipe system (Figure 2). The fluidization filter is a combination of three meshes. The top and bottom layers are fine and coarse stainless steel meshes, respectively, which protects and supports the middle layer; the middle layer is a fine Nylon mesh with an opening size of 41 micro-meters which functions as a filter. The pipe system has 8 parallel pipes with an inner diameter of 4 mm and each of which has 50 evenly distributed holes. The total area of the holes on each pipe is smaller than the inner cross section area of the pipe. In order to provide evenly distributed fluid pressure in the fluidization system, the holes are facing downwards. The transverse pipe and two valves link the parallel pipes inside the strongbox and the fluid reservoir outside of the strongbox via a pump.

A sample was made by the fluidisation method, i.e. by pumping de-aired fluid. After around 180 seconds of fluidization, the inlet was stopped to let the sand grains settle down and form a loose layer. The relative density of the sample was calculated based on the total sand mass and total sample volume. The fluid surface was 180 mm (model scale) above the fluidization filter.

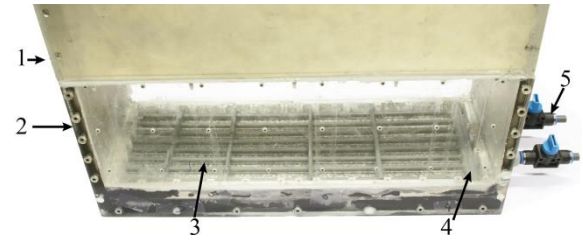

Figure 2. Fluidization system: 1) extension box; 2)strongbox; 3) parallel pipes; 4) transverse pipe; 5) valves

3 TILTING DEVICE FOR TRIGGERING STATIC LIQUEFACTION

A tilting device has been built for simulating submerged sand slope liquefaction triggered by the increase of slope angle. As shown in Figure 3, it is composed of an outer frame, a base plate, five bearing blocks, six shaft block and a rotating axis. By lifting up one side of the frame using a linear motor (Figure 4**Error! Reference source not found.**, Linak 282100-40150100, capacity: 1 kN), the whole strongbox can rotate. A relatively low force is required for tilting the strongbox since the rotating axis is located in the middle of the sample, hence it carries most of the weight. The maximum tilting angle is 22º.

The highest and lowest tilting rates are 2.0 °/s and 0.1 °/s, at model scale, respectively.

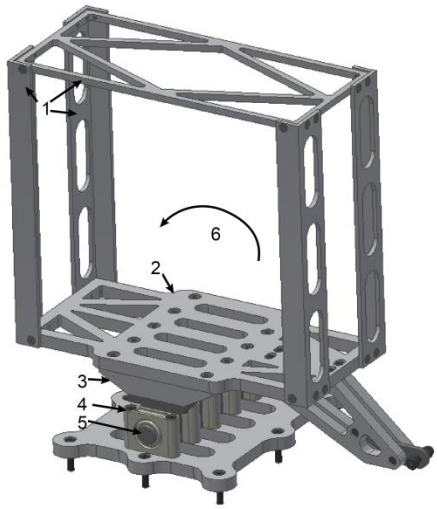

Figure 3. Schematic sketch of the newly developed tilting frame for triggering static liquefaction for the geo-centrifuge at TU Delft: 1) outer frame; 2) base plate; 3) bearing blocks; 4) shaft blocks; 5) rotating axis; 6) rotating direction

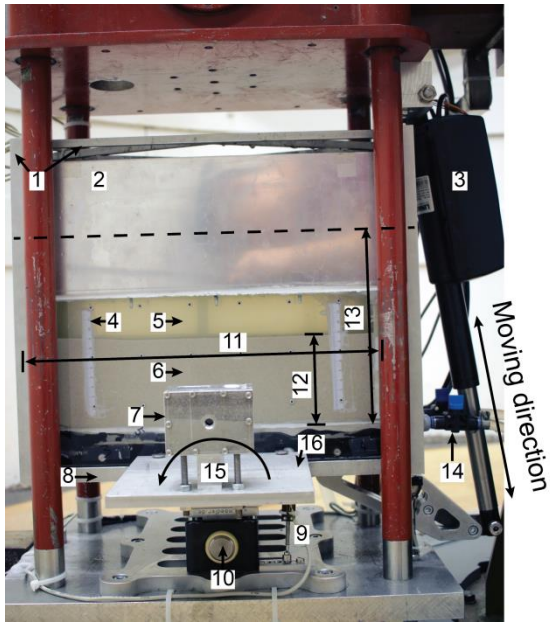

Figure 4. Front view of test setup after sample preparation (model scale): 1) outer frame; 2) extension box; 3) linear motor; 4) scaler; 5) viscous fluid; 6) submerged sand; 7) high resolution, high speed camera; 8) base plate; 9) linear potentiometer; 10) rotating axis; 11) sample length: 355 mm; 12) sample thickness: 87 mm; 13) fluid height: 180 mm; 14) valves; 15) tilting direction; 16) camera holder

Before fluidizing the sample, the strongbox filled with de-aired fluid and sand was installed inside the tilting frame as shown in Figure 4. A potentiometer (S13FLP25A) was installed to monitor the tilting angle during the test. A high speed camera can record the field of displacement.

4 SAND AND PORE FLUID

4.1 Sand material

A sub-rounded industrial sand, also known as Geba Sand, was used in this study. The coefficients of uniformity and curvature are 1.55 and 1.24, respectively. The minimum and maximum void ratios are 0.64 and 1.07, respectively. The grain diameter at 50% passing (D_{50}) is 0.117 mm. The permeability is 4.2 x 10^{-5} m/s. The residual friction angle is 36° (Maghsoudloo et al. 2018).

4.2 Pore fluid

Viscous fluid as the submerging fluid is needed in order to simulate static liquefaction at N*g* acceleration condition. Static liquefaction can be induced by sudden increase of pore pressure. One of the possible internal mechanisms for this is the collapse of the voids filled with fluid happening at grain scale (Askarinejad et al. 2014). Considering the scaling factors for generation (Equation 1) and dissipation time of excess pore pressure (Equation 2) at grain scale, Askarinejad et al. (2014) proposed that the viscosity of the fluid should be $\sqrt{N}$-times more than water for a sample, which is N-times

smaller than prototype, tested at N*g* acceleration condition,

$$T_r^{generation} = \frac{T_p^{generation}}{T_m^{generation}} = \sqrt{\mathrm{N}} \quad (1)$$

$$T_r^{dissipation} = \frac{T_p^{dissipation}}{T_m^{dissipation}} = \mathrm{N} \quad (2)$$

where, $T^{generation}$ is the time scale for the generation of excess pore pressure caused by the gravitational falling of a particle at grain scale, $T^{dissipation}$ is the time scale for the dissipation of excess pore pressure obtained from Darcy's law at grain scale, the subscripts *p* and *m* stand for prototype and model, respectively, and the subscript *r* represents the scaling ratio (prototype/model).

Therefore, de-aired fluid with a kinematic viscosity of $\sqrt{\mathrm{N}} = 3.3$ cSt, where N is 10 in this study. The viscous fluid was made of E10M Hydroxypropyl Methylcellulose (HPMC) powder.

5 CENRIFUGE TESTS

A centrifuge test was performed with a tilting rate of 0.1 °/s at model scale which is equivalent to 0.01 °/s at prototype scale, since the dynamic time scaling factor (prototype/model) is N. The sample was made very loose initially at 1*g* condition with a relative density ($Dr_{\_1g}$) of 18%; however, the relative density at 10g condition ($Dr_{\_10g}$) increased to 29% as a result of increasing of stress level. The sand layer thickness was 0.83 m at 10g at prototype scale. The details of the test are listed in Table 1. Furthermore, Cent2 was done without sand and the strongbox was filled only with the de-aired viscous fluid.

The readings of the PPTs for test Cent2 show the hydrostatic fluid pressure change during the tiling process. Hence the excess pore fluid pressures at three PPTs' locations of test Cent1 can be obtained by subtracting hydrostatic fluid pressures from the test results of Cent1. The change of excess pore fluid pressure for test Cent1 is shown in Figure 5**Error! Reference source not found.**. The submerged slope failed at an angle of 17.7°. It can be seen that the excess pore fluid pressure increased abruptly and simultaneously, which indicates the occurrence of liquefaction. It took around 1.6 seconds (Equation 1), at prototype scale, for the excess pore pressures to reach a peak. The images taken by the high speed camera during the tilting show that the sand liquefied in a very sudden manner which corresponds with the PPTs' readings.

Table 1. Summary of the centrifuge test specifications

Test Name	Tilting rate (°/s, prototype scale)	$Dr_{\_1g}$ (%)	$Dr_{\_10g}$ (%)	Failure angle (°)
Cent1	0.01	23	34	17.7
Cent2	0.01	-	-	-

The maximum excess pore pressures are 1.95 kPa, 1.80 kPa and 1.90 kPa for the sensors PPT1, PPT2 and PPT3, respectively (see Figure 1). PPT1 measured the maximum excess pore pressure which was placed at the bottom of the sample, near the slope toe during the tilting. The excess pore pressures from all sensors before liquefaction are negative which means that the bottom layer of the sand was dense, therefore dilation happened at this level while the sample was being tilted.

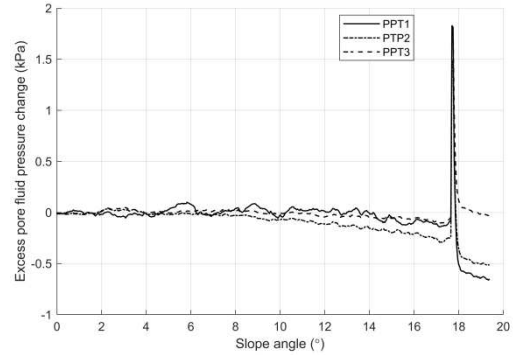

Figure 5. Changes in excess pore water pressure for Cent1

6 CONCLUSIONS

A new strongbox was designed and constructed with an integrated fluidization system. This system was used to prepare a saturated loose sand sample. A novel actuator was introduced which enables the authors to simulate the phenomenon when the slope inclination increases due to scouring effect or dredging. A saturated loose sand sample with a sand layer thickness of 0.83 m at prototype scale was made directly in the centrifuge carrier and was triggered to liquefaction at a g-level of 10 by gradually elevating the slope angle with a rate of 0.01°/s at prototype scale. The selected submerging fluid was 3.2 times more viscous than water. Liquefaction happened within 1.6 seconds at prototype scale.

It can be concluded that scouring effect induced liquefied landslides can be simulated in centrifuge. Submarine slopes can statically liquefy in a very short time and show no excess pore pressure or measurable physical deformation before failure.

7 ACKNOWLEDGEMENTS

The technical support from J.J. de Visser, Kees van Beek, Ronald van Leeuwen, Leon Roessen, Bert Bakker and Tom Philips is gratefully acknowledged. The first author is financially supported by China Scholarship Council.

8 REFERENCES

[1] Askarinejad, A., Beck, A. & Springman, S.M. (2014). Scaling law of static liquefaction mechanism in geocentrifuge and corresponding hydromechanical characterization of an unsaturated silty sand having a viscous pore fluid. *Canadian Geotechnical Journal,* 52(6): 708-720, doi:10.1139/cgj-2014-0237.

[2] Askarinejad, A., Zhang, W., de Boorder, M. & van der Zon, J. (2018). Centrifuge and numerical modelling of static liquefaction of fine sandy slopes,*Physical Modelling in Geotechnics, Volume 2* (pp. 1119-1124), CRC Press (Pub).

[3] Byrne, P., Puebla, H., Chan, D., Soroush, A., Morgenstern, N., Cathro, D., Gu, W., Phillips, R., Robertson, P. & Hofmann, B. (2000). CANLEX full-scale experiment and modelling. *Canadian geotechnical journal,* 37(3): 543-562.

[4] Chu, J., Leroueil, S. & Leong, W.K. (2003). Unstable behaviour of sand and its implication for slope stability. *Canadian Geotechnical Journal,* 40: 873-885.

[5] De Groot, M., Lindenberg, J., Mastbergen, D. & Van den Ham, G. (2012). Large scale sand liquefaction flow slide tests revisited. In *Eurofuge 2012*, Delft, The Netherlands, 1-22.

[6] De Jager, R.R. (2018). *Assessing Liquefaction Flow Slides: Beyond Empiricism.* Delft University of Technology, Delft.

[7] De Jager, R.R., Maghsoudloo, A., Askarinejad, A. & Molenkamp, F. (2017). Preliminary results of instrumented laboratory flow slides. In *Proceedings of the 1st International Conference on the Material Point Method* 175:212-219, doi:10.1016/j.proeng.2017.01.012.

[8] Della, N., Arab, A., Belkhatir, M. & Missoum, H. (2009). Identification of the behavior of the Chlef sand to static liquefaction. *Comptes Rendus Mécanique,* 337(5): 282-290.

[9] Jefferies, M. & Been, K. (2006). *Soil liquefaction: a critical state approach*. Taylor & Francis Group (Pub), Lond

[10] Kvalstad, T., Nadim, F. & Arbitz, C. (2001). Deepwater geohazards: geotechnical concerns and solutions. In *Offshore Technology Conference*, Offshore Technology Conference.

[11] Lade, P.V. (1992). Static instability and liquefaction of loose fine sandy slopes. *Journal of Geotechnical Engineering,* 118(1): 51-71.

[12] Maghsoudloo, A., Askarinejad, A., de Jager, R., Molenkamp, F. & Hicks, M. (2018). Experimental investigation of pore pressure and acceleration development in static liquefaction induced failures in submerged slopes,*Physical Modelling in Geotechnics, Volume 2* (pp. 987-992), CRC Press (Pub).

[13] Maghsoudloo, A., Galavi, V., Hicks, M.A. & Askarinejad, A. (2017). Finite element simulation of static liquefaction of submerged sand slopes using a multilaminate model. In *19th International Conference on Soil Mechanics and Geotechnical Engineering*, Seoul, 2:805-808.

[14] Masson, D., Harbitz, C., Wynn, R., Pedersen, G. & Løvholt, F. (2006). Submarine landslides: processes, triggers and hazard prediction. *Philosophical Transactions of the Royal Society of London A: Mathematical, Physical and Engineering Sciences,* 364(1845): 2009-2039.

[15] Rietdijk, J., Schenkeveld, F., Schaminée, P. & Bezuijen, A. (2010). The drizzle method for sand sample preparation. In *Proceedings of the International Conference on Physical Modelling in Geotechnics 2010 (ICPMG 2010)*, Zurich, Switzerland, CRC Pres, 267-272.

[16] Sassa, S. & Sekiguchi, H. (1999). Wave-induced liquefaction of beds of sand in a centrifuge. *Geotechnique,* 49(5): 621-638.

[17] Silvis, F. & Groot, M.d. (1995). Flow slides in the Netherlands: experience and engineering practice. *Canadian geotechnical journal,* 32(6): 1086-1092.
[18] Spence, K. & Guymer, I. (1997). Small-scale laboratory flowslides. *Geotechnique,* 47(5): 915-932.
[19] Vaid, Y.P., Sivathayalan, S. & Stedman, D. (1999). Influence of specimen-reconstituting method on the undrained response of sand. *Geotechnical Testing Journal,* 22(3): 187-195, doi:10.1520/GTJ11110J.